Current Applied Physics 12 (2012) 637–642

Contents lists available at SciVerse ScienceDirect

Current Applied Physics

journal homepage: www.elsevier.com/locate/cap

Difference of dispersion behavior between graphene oxide and oxidized carbon nanotubes in polar organic solvents

Do Hyeong Kim, Young Soo Yun, Hyoung-Joon Jin*

Department of Polymer Science and Engineering, Inha University, Incheon 402-751, Republic of Korea

ARTICLE INFO

Article history:
Received 2 June 2011
Received in revised form
11 August 2011
Accepted 17 September 2011
Available online 2 October 2011

Keywords:
Graphene oxide
Carbon nanotube
Hansen solubility parameter

ABSTRACT

This study examined the dispersion behavior of graphene oxide (GO) and oxidized carbon nanotubes (o-CNT) in a polar solvent, as well as the differences in the behavior related to the Hansen solubility parameter windows. In polar aprotic solvents, GO and o-CNT showed similar dispersion behavior. On the other hand, in polar protic solvents, such as ethanol and isopropanol, GO did not show dispersion stability whereas the o-CNTs did. This difference in the dispersion behavior between GO and o-CNTs resulted from the stronger hydrogen bonding between the GO interlayer induced by a large amount of oxygen functional groups and flexible two-dimensional morphology with a large surface area.

1. Introduction

Graphene is a new class of two-dimensional carbon nanostructure that has attracted tremendous attention owing to its unique physical, chemical, and mechanical properties [1–6]. Graphene has high mechanical strength (>1060 Gpa), high thermal conductivity (~3000 W/m K), high electron mobility (15000 cm^2/V s) and high specific surface area (2600 m^2/g) [2–5]. The unique nanostructure and properties hold great promise for potential applications. Graphene oxide (GO), consisting of two-dimensional oxidized graphene sheets, can be exfoliated easily using Hummers method [2]. GO can be dispersed easily in polar organic solvents due to a large number of functional groups on the surface, such as carboxylic acid, hydroxyl and epoxide groups [3–5]. The dispersion behavior of GO in a range of polar organic solvents can be characterized using the Hansen solubility parameter, which consists of the atomic dispersion force, permanent dipole–permanent dipole force and hydrogen bonding force [6]. Recently, many groups reported polar solvent windows of reduced GO determined by the sum of the polarity cohesion (δ_P) and hydrogen bonding cohesion (δ_H) factors of the Hansen solubility parameter. Coleman et al. measured the dispersibility of graphene in 40 solvents. They reported that good solvents for graphene are characterized by the Hansen solubility parameter [6]. Ruoff et al. obtained homogeneous colloidal suspensions of graphene oxide in a wide range of organic solvent systems [7]. As a result, only solvents with ($\delta_P + \delta_H$) in a range of 13–29 were found to yield stable reduced GO suspensions. In the case of GO, its Hansen solubility parameter windows would be larger than those of reduced GO. On the other hand, there are no reports related to the polar solvent windows of GO.

Carbon nanotubes (CNTs), which consist of a rolled graphene sheet or sheets, have been one of the most extensively researched materials. This attention derives from their high elasticity and tensile strength, outstanding electrical and thermal conductivity, and good thermal stability and chemical resistance [8–11]. CNTs have accordingly found a range of applications, such as nanoelectronics, sensors, nanocomposites, batteries, supercapacitors, and hydrogen storage devices. Nevertheless, the application of CNTS greatly depends on their dispersion stability.

The dispersion stability of CNTs is essential to counterbalance the van der Waals and π–π stacking interaction. Physical and chemical approaches are currently being pursued to disperse and exfoliate CNTs [9]. Acid treatments of CNTs by a mixture solution of sulfuric acid and nitric acid have been used to purify and functionalize the MWCNTs. Oxidized CNTs (o-CNTs) have a large amount of oxygen groups on their surface, such as carboxylic acid and hydroxyl and epoxide groups, such as in GO [10]. In the case of CNTs, there are many reports showing that they can be dispersed in polar solvents, such as dimethylformamide (DMF), dimethyl sulfoxide (DMSO), and N-methylpyrrolidone (NMP) [11,12]. On the other hand, there are no reports related to the polar solvent windows of o-CNT.

* Corresponding author. Tel: +82 32 860 7483; fax: +82 32 865 5178.
E-mail address: hjjin@inha.ac.kr (H.-J. Jin).

1567-1739/$ – see front matter © 2011 Elsevier B.V. All rights reserved.
doi:10.1016/j.cap.2011.09.015

In this study, GO and o-CNT are similar allotropes of carbon with acidic functional group. This study investigated the difference in dispersion behavior of GO and o-CNTs in selectivity polar protic solvents as well as the differences in the behavior in relation to the Hansen solubility parameter windows. Owing to hydrogen bonding between the interlayer, GO and o-CNT show different interactions in polar protic solvents. The results suggest that the strength of interlayer hydrogen bonding will be attenuated, possibly allowing for dispersion in polar protic solvents.

2. Experimental section

2.1. Materials

The graphite powder was purchased from Sigma-Aldrich (Product Number 332461). The MWCNTs (JEIO Co., Incheon, Korea) were synthesized by thermal chemical vapor deposition (CVD). Dispersions of exfoliated graphene oxide and oxidized CNT (o-CNT) were prepared in a range of polar solvents (purchased from Sigma-Aldrich).

2.2. Preparation of graphene oxide

The graphene oxide was prepared from natural graphite powder using the Hummers method. Natural graphite (1 g) and $NaNO_3$ (0.5 g) were stirred into 70 mL of H_2SO_4 at room temperature. Subsequently, $KMnO_4$ (3 g) was added slowly into the mixture with stirring. After ultrasonicating the mixture solution for 15 min and stirring for 90 min at room temperature, it was poured into 600 ml of de-ionized water, which was followed by the addition of 300 ml of a 10% H_2O_2 solution. The as-obtained graphite oxide slurry was exfoliated to graphene oxide by ultrasonication using an ultrasonic generator (Kodo Technical Research, Korea) with a nominal frequency and power of 28 kHz and 600 W, respectively, for 3 h at 25 °C. The mixture was filtered and washed three times with a 10% HCl solution to remove the metal ions. The product was washed three times with acetone and de-ionized water each to remove the acidic or ionic impurities, and then dried in a vacuum oven at 60 °C [4,13].

2.3. Preparation of oxidized CNTs

The o-CNTs were treated with strong acid using the following typical procedure. First, the CNTs were treated with a concentrated H_2SO_4/HNO_3 (3/1 v/v) solution at 60 °C for 6 h. The oxidized CNTs were washed several times with de-ionized water using a nylon membrane filter (0.45 μm) and dried overnight in a vacuum oven at 60 °C.

2.4. Preparation of GO and oxidized CNTs dispersion in different polar solvents

The dried GO and o-CNTs were first ground with a mortar and pestle, added to the solvent and sonicated in an ultrasound bath cleaner (Kodo Technical Research, Korea) for 1 h. To allow direct comparisons between the dispersing behaviors of the different solvents, a certain amount of graphene oxide or oxidized CNTs was added to a given volume of solvent in such a way that the resulting nominal concentration was adjusted to 0.01 wt % for all solvents. The GO or o-CNTs dispersions were tested in the following organic polar solvents for 10 days: acetone, methanol, ethanol, isopropanol, ethylene glycol, acetic acid, dimethyl sulfoxide (DMSO), N,N-dimethylformamide (DMF), N-methyl-2-pyrrolidone (NMP), tetrahydrofuran (THF) and acetonitrile. In all solvents, the amount of water was <0.1% because the common solvent for the preparation of GO and o-CNTs dispersions is water. Aqueous dispersions of the

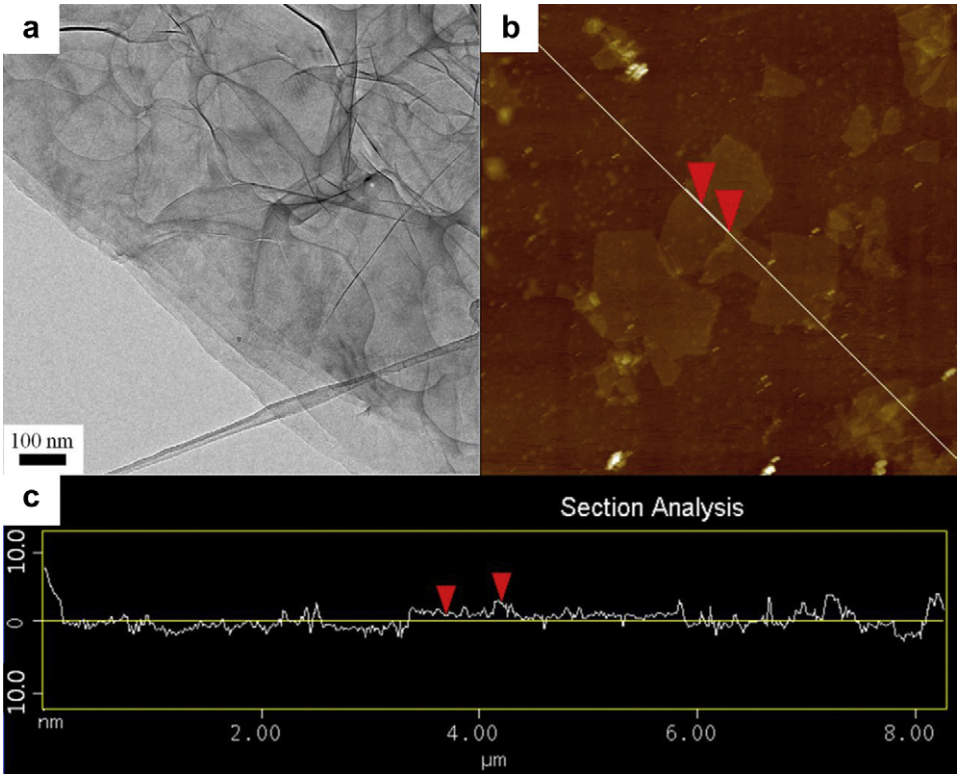

Fig. 1. High-resolution TEM image clearly displays the dispersion of several GO layers in solution (a). The scale bar is 6 μm (b, c) AFM image the mean thickness of flat nanosheet is 3 nm.

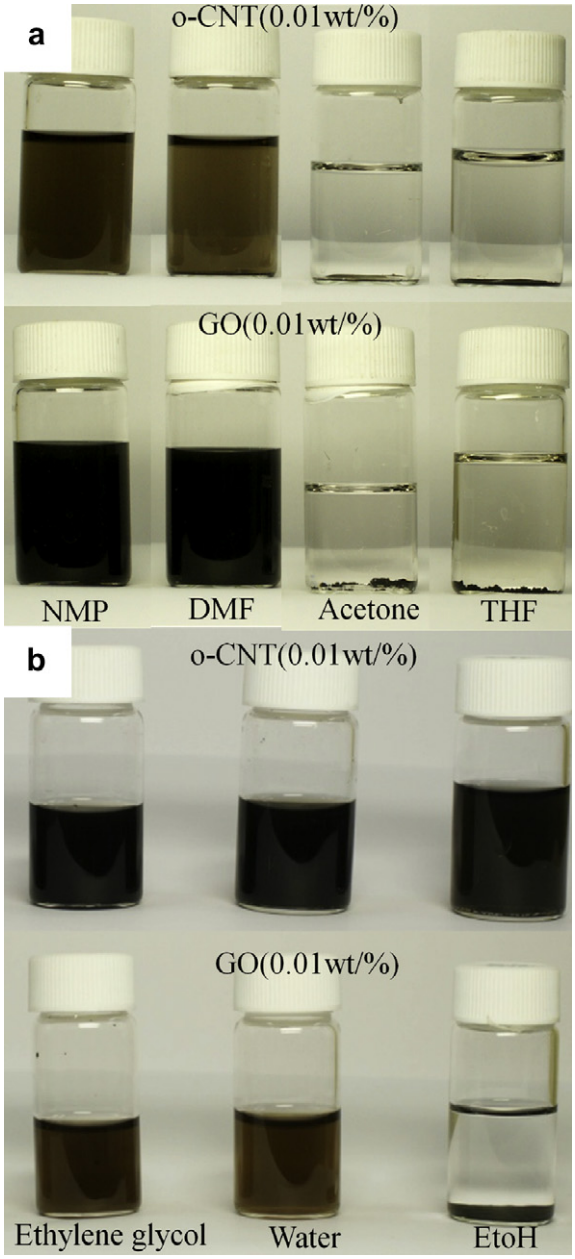

Fig. 2. Digital photo images of (a) the GO and o-CNT in aprotic solvent (NMP, DMF, Acetone, THF), (b) the GO and o-CNTs in protic solvent (diethylene glycol, water, ethanol).

as-prepared GO and o-CNTs were also prepared under the same conditions as those used in the case of the organic polar solvents. The aqueous dispersions served as a reference against which the organic polar solvent dispersions were compared.

Table 1
Dispersion stability of GO and o-CNTs in polar aprotic solvents (THF, Acetone, DMF, NMP, DMSO) along with electrostatic information.

Solvent	$\delta_P + \delta_H$	Dipole moment	Dispersion GO/o-CNT
THF	13.7	1.75 D	NO/NO
Acetone	17.4	2.88 D	NO/NO
DMF	26	3.82 D	**YES**/**YES**
NMP	19.5	4.09 D	**YES**/**YES**
DMSO	26.6	3.96 D	**YES**/**YES**

Table 2
Dispersion stability of GO and o-CNTs in polar protic solvents (Diethylene glycol, IPA, ethanol, acetic acid, water) along with electrostatic information.

Solvent	$\delta_P + \delta_H$	Dipole moment	Dispersion GO/o-CNT
Diethylene glycol	32.7	2.28 D	**YES**/**YES**
Isopropanol (IPA)	22.5	1.66 D	NO/NO
Ethanol	28.2	1.69 D	NO/**YES**
Acetic acid	21.5	1.74 D	NO/NO
Water	58.3	1.85 D	**YES**/**YES**

2.5. Characterization

Field-emission transmission electron microscopy (TEM, CM200, Philips, Netherlands) was used to confirm the presence of graphene nanoparticles, and the samples were prepared by drop casting the dispersion onto holey carbon grids. The morphology observation and thickness measurement was performed using a AFM (Autoprobe CP, park scientific Instruments, USA). Turbiscan analysis (Formulaction, France) exhibited dispersion stabilities of o-CNTs and GO dispersions in ethanol. The structure of the GO and o-CNTs was examined by X-ray photoelectron spectroscopy (XPS, PHI 5700 ESCA spectrometer) with monochromated Al Kα radiation (hv = 1486.6 eV). The stability of GO and o-CNTs in the polar solvents through electrostatic repulsion was characterized by the zeta potential (electrophoretic light scattering ELS-8000, Otsuka, Japan). Quantitative analysis of the atomic content of the GO and o-CNTs was identified by elemental analysis (EA) (Ceinstruments Thermo EA1112, England).

3. Results and discussion

Fig. 1 shows the morphology of the graphene oxide (GO). GO had lateral dimensions of several micrometers and a thickness of 2 nm, which is characteristic of fully exfoliated GO, as shown by TEM and atomic force microscopy (AFM) [3]. The GO and as-prepared oxidized CNT (o-CNTs) were dispersed in water and 8 types of polar solvents to a nominal concentration of 0.1 wt% with the aid of

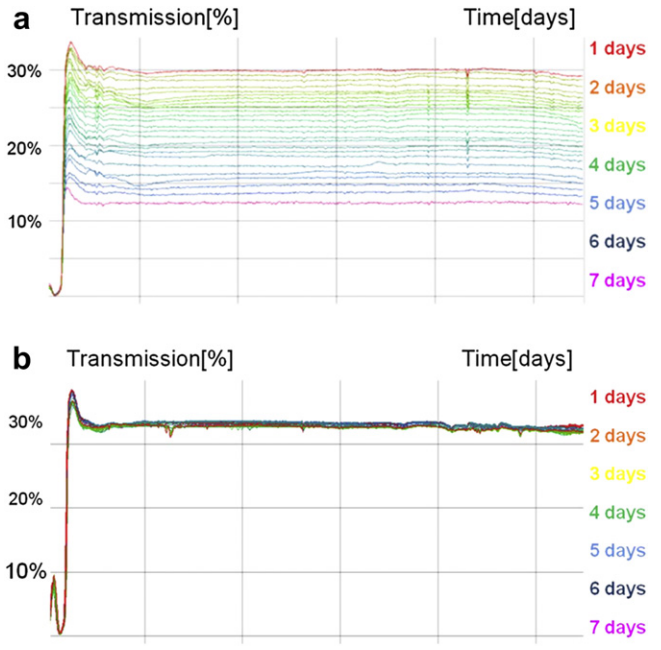

Fig. 3. Turbiscan data of (a) the GO dispersion (0.01 mg/mL) in ethanol and (b) the o-CNT dispersion (0.01 mg/mL) in ethanol.

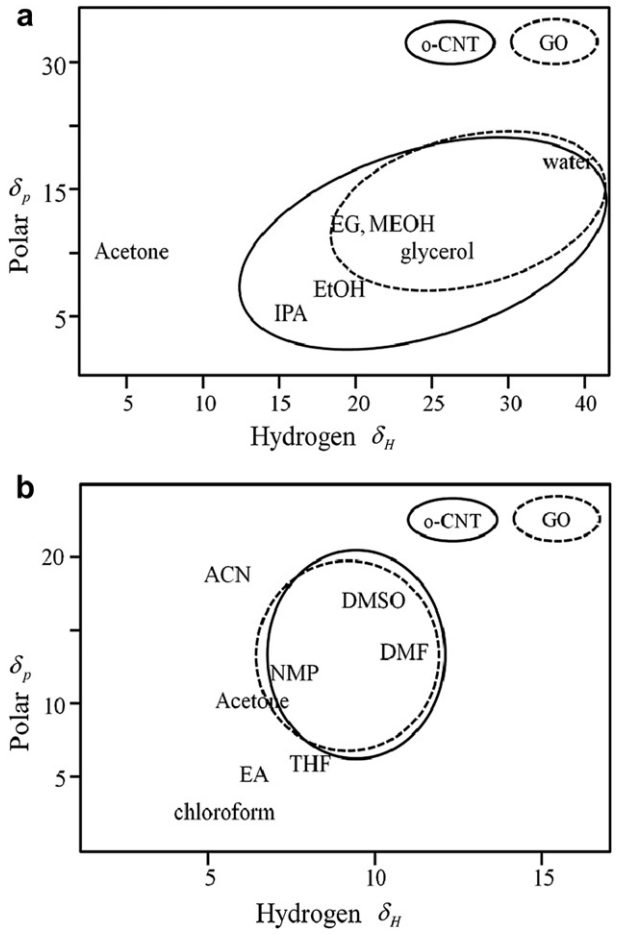

Fig. 4. Hansen solubility windows of GO and o-CNT in (a) polar protic organic solvents and (b) polar aprotic organic solvents.

bath ultrasonication for 3 h, and the dispersions were then allowed to settle for one week. Fig. 2 shows digital pictures of GO and o-CNTs of the dispersion in polar organic solvents for one week after ultrasonication. GO and o-CNTs could be dispersed in the same aprotic solvent (Fig. 2a) (THF, Acetone, DMF and NMP). On the other hand, the dispersion of GO and o-CNTs showed different behavior with respect to the type of protic solvents in Fig. 2b. The vials with GO in ethanol contained visible precipitates, indicating poor dispersion. On the other hand, the dark dispersion of o-CNTs in ethanol, ethylene glycol and water showed no visible precipitate and was stable for weeks.

Table 1 lists the dispersion stability of GO and o-CNTs in selected aprotic solvents as well as the Hansen solubility parameter ($\delta_P + \delta_H$) and dipole moment of aprotic solvents [7,10]. Those characteristics of aprotic solvents strongly interacted with the dispersion of solute. The dispersion behavior of GO and o-CNT were similar and they showed good dispersion stability in aprotic solvents with a high dipole moment (>3.82 D). For aprotic solvents with a substantial dipole moment (>3.82 D), dipole–solute interactions often dominate during solvation, accounting for more than 80% of the total interaction in many cases [14].

Table 2 lists the dispersion behavior in selected protic solvents. The degree of hydrogen bonding in protic solvents could determine the dispersion behavior of the solute. In the case of o-CNT, the dispersion stability was high in the solvents with ($\delta_P + \delta_H$) in a wide range of 19–58. In contrast to o-CNT, GO did not display dispersion stability in ethanol (EtOH, $\delta_P + \delta_H = 28.2$) or isopropanol (IPA, $\delta_P + \delta_H = 22.5$) [7]. Therefore, the solvent range, wherein GO has dispersion stability, is not correlated linearly with the $\delta_P + \delta_H$ value.

The stability of the GO and o-CNT dispersed in ethanol were characterized by a multiple light scattering (Turbiscan). Fig. 3a shows that no sedimentation in the o-CNTs/ethanol dispersion occurred over a 1 week period. In the back scattering profiles, the curves of the o-CNTs dispersion in the ethanol were constant with time. On the other hand, those of the GO dispersion in ethanol increased rapidly (Fig. 3b). The o-CNTs dispersion prepared in ethanol appeared to be more stable than the GO dispersion prepared in ethanol. This difference was attributed to the stronger hydrogen bonding between the GO interlayer induced by the large number of oxidation groups and flexible two-dimensional morphology with a large surface area.

Table 3
Elemental analysis of Graphite, CNT, Graphene oxide, oxidized CNTs show a C/H/O/N ratio.

Elemental	C	H	O
CNT	97.16	–	0.3
Graphite	94.51	–	1.67
o-CNT	87.25	0.55	12.20
Graphene oxide	38.4	2.53	57.9

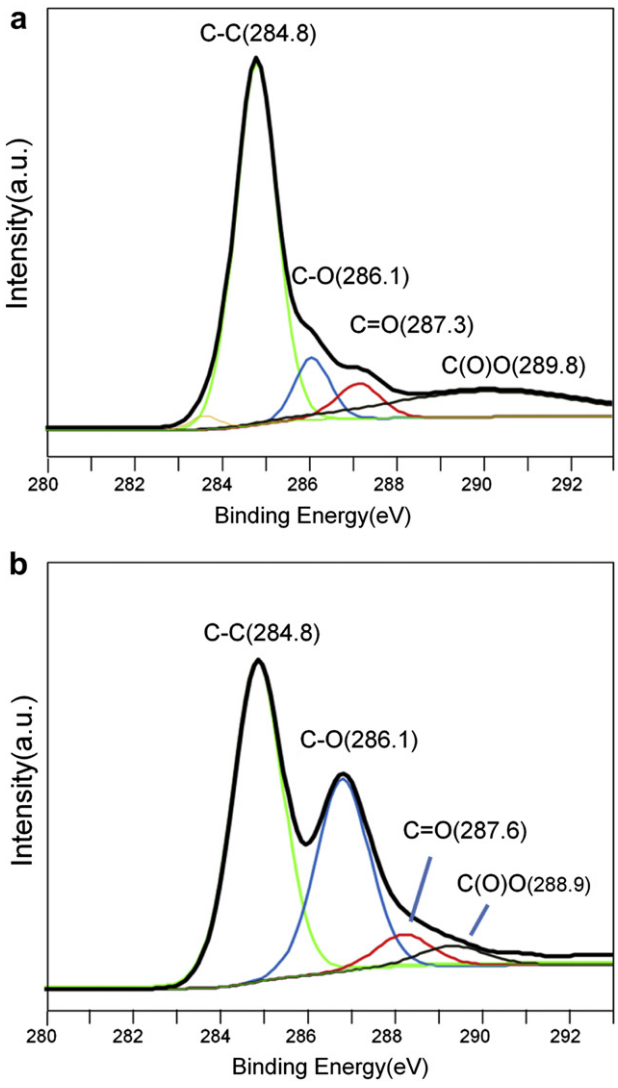

Fig. 5. High-resolution core-level C 1s XP spectra of the Graphene oxide (a) and the o-CNT (b).

Fig. 4a, b shows the Hansen solubility diagrams using only δ_P and δ_H used to measure the dispersion in polar solvents. The "solubility sphere" was adjusted so that all solvents lie within it and all non-solvents lie outside of it. Although GO and o-CNT have a similar Hansen solubility sphere in aprotic solvents, o-CNT has a larger sphere than GO in protic solvents. This result was identical to the experimental results.

This difference in the dispersion behavior between GO and o-CNT results from the degree of oxidation and morphological differences between them [3]. Therefore, the degree of oxidation of GO and o-CNT were calculated using the results from elemental analysis, as listed in Table 3. A C:O ratio of 87.2:12.2 was measured for o-CNT by elemental analysis, compared to 38.4:57.9 for GO. Fig. 5 shows the XP spectra of GO [15] and o-CNT [16]. The XPS peaks of GO and o-CNT were assigned to one main C–C and three small C–O components, which were observed in the C1s peaks of the GO and o-CNT; C–C (284.6 eV) for sp^2 carbon; C–O (286.1 eV); C]O (287.3 eV); C(O)O (289.8 eV). The peak intensities and atomic ratios (O/C) of o-CNTs in the C1s peaks clearly decreased compared to those of GO, and a large amount of oxygen functional group was incorporated on the surface of GO compared to the o-CNT. Therefore, hydrogen bonding between oxidized carbon materials and solvents differ according to amount of oxygen functional groups [17].

Fig. 6 proposes a schematic model of hydrogen bonding between the GO interlayer and between the o-CNT interlayer. GO with a large number of oxidation groups is relatively advantageous for hydrogen bonding between the GO interlayer. Furthermore, the flexible two-dimensional morphological characteristics of GO with a large surface area are advantageous for hydrogen bonding between the GO interlayer compared to hydrogen bonding between GO and the solvent [3,18]. Therefore, EtOH and IPA, which do not have a strong dipole moment or strong hydrogen bonding interaction, cannot readily solvate GO. This accounts for the change in dispersion behavior between GO and o-CNT in some solvents, such as EtOH and IPA, despite they both having a sp^2 carbon structure.

Fig. 7 shows the zeta potential of GO and o-CNT dispersed in selected polar solvents [19–21]. All zeta potentials of o-CNTs in the selected polar solvents were higher than that of GO. Although

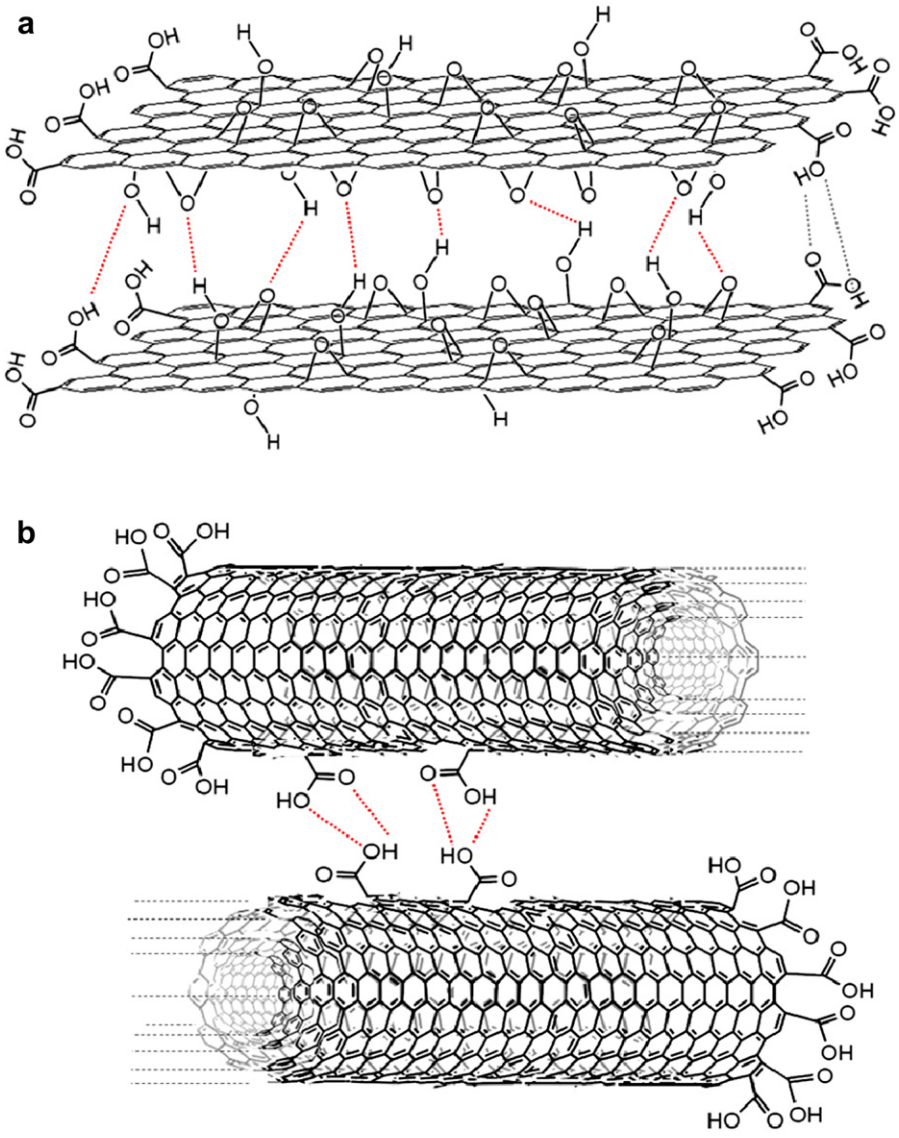

Fig. 6. Scheme showing the hydrogen bonding interaction between the GO interlayer (a) and o-CNT interlayer (b).

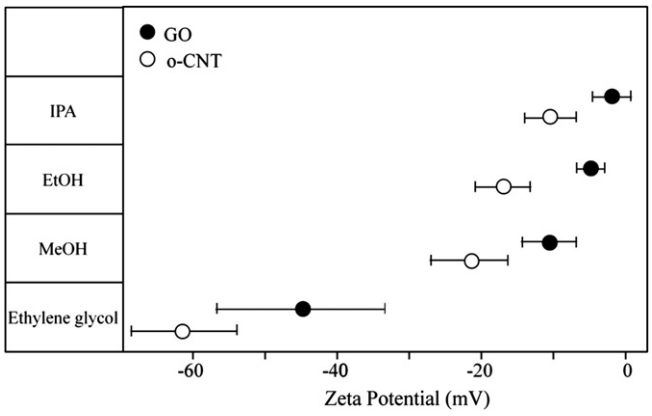

Fig. 7. The ζ-potential distribution of o-CNT and GO in polar aprotic solvents (isopropanol, ethanol, methanol, ethylene glycol, water). The o-CNT and GO concentration is 0.01 wt% in solvents.

relatively more oxidation groups are incorporated on the GO surface, its zeta potential was lower than that of o-CNTs. This is due to the strong interaction induced by the hydrogen bonding force between the GO interlayer, which obstructs the mobility of GO in the solvents [3]. In particular, the zeta potential of GO in EtOH and IPA is <-10 mV, which is the lower limit for the dispersion stability of GO in a solvent.

4. Conclusions

The dispersion stability of GO and o-CNT in polar organic solvents was compared. GO and o-CNT were similar and they showed good dispersion stability in aprotic solvents with a high dipole moment. On the other hand, GO and o-CNT were dispersed in selected protic solvents. In contrast to GO, o-CNT has good dispersion stability in ethanol. This difference was attributed to the stronger hydrogen bonding between the GO interlayer induced by the large number of oxidation groups and the flexible two-dimensional morphology with a large surface area. The dispersion behavior of GO and o-CNT were confirmed by zeta potential analysis and multiple light scattering (turbiscan). In addition, the Hansen solubility parameter sphere reflected the characteristics of polar solvents that can disperse GO or o-CNT.

Acknowledgements

This work was financially supported by a grant from the Fundamental R&D Program for Core Technology of Materials funded by the Ministry of knowledge Economy, Republic of Korea.

References

[1] S.V. Tkachev, E.Y. Buslaeva, S.P. Gubin, Inorg. Mater. 47 (2011) 1–10.
[2] W.S. Hummers, R.E. Offeman, J. Am. Chem. Soc. 80 (1958) 1339.
[3] S. Stankovich, R.D. Piner, S.T. Nguyen, R.S. Ruoff, Carbon 44 (2006) 3342–3347.
[4] I.K. Moon, J. Lee, R.S. Ruoff, H. Lee, Nat. Commun. 1 (2010) 1067.
[5] J.I. Paredes, S.V. Rodil, A.M. Alonso, J.M.D. Tascón, Langmuir 24 (2008) 10560–10564.
[6] Y. Hernandez, M. Lotya, D. Rickard, S.D. Bergin, J.N. Coleman, Langmuir 26 (2010) 3208–3213.
[7] S. Park, J. An, I. Jung, R.D. Piner, S.J. An, X. Li, A. Velamakanni, R.S. Ruoff, Nano. Lett. 9 (2009) 1593–1597.
[8] L. Qiao, W.T. Zheng, Q.B. Wen, Q. Jiang, Nanotechnology 18 (2007) 155707.
[9] M.D. Clark, R. Krishnamoorti, J. Phys. Chem. C 113 (2009) 20861–20868.
[10] J. Lee, M. Kim, C.K. Hong, S.E. Shim, Meas. Sci. Technol. 18 (2007) 3707–3712.
[11] D.S. kim, D. Nepal, K.E. Geckeler, Small 1 (2005) 1117–1124.
[12] H.T. Ham, Y.S. Choi, I.J. Chung, J. Colloid Interface. Sci. 286 (2005) 216–223.
[13] J.E. Kim, T.H. Han, S.H. Lee, J.Y. Kim, C.W. Ahn, J.M. Yun, S.O. Kim, Angew. Chem. 50 (2011) 3043–3047.
[14] L. Reynolds, J.A. Gardecki, S.J.V. Frankland, M.L. Horng, M. Maroncelli, J. Phys. Chem. 100 (1996) 10337–10354.
[15] X. Qi, K.Y. Pu, X. Zhou, H. Li, B. Liu, F. Boey, W. Huang, H. Zhang, Small 6 (2010) 663–669.
[16] S. Kundu, Y. Wang, W. Xia, M. Muhler, J. Phys. Chem. C 112 (2008) 16869–16878.
[17] S.H. Lee, J.S. Park, C.M. Koo, B.K. Lim, S.O. Kim, Macromol. Res. 16 (2008) 261–266.
[18] E.-Y. Choi, T.H. Han, J. Hong, J.E. Kim, S.H. Lee, H.W. Kim, S.O. Kim, J. Mater. Chem. 20 (2010) 1907–1912.
[19] L. Zhao, L. Gao, Colloid. Surf. A 224 (2003) 127–134.
[20] K.T. Jeng, C.C. Chien, N.Y. Hsu, S.C. Yen, S.D. Chiou, S.H. Lin, W.M. Huang, J. Power Sources 160 (2006) 97–104.
[21] P. Kumar, S. Karmakar, H.B. Bohidar, J. Phys. Chem. C 112 (2008) 15113–15121.